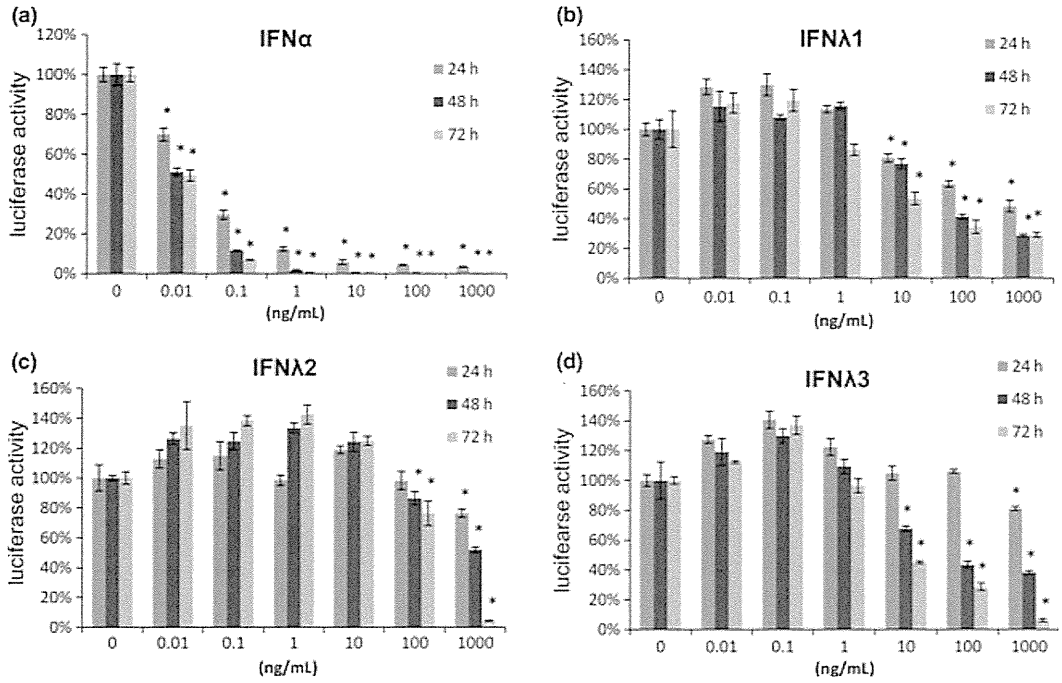

Fig. 1 IFN-α and IFN-λs inhibit HCV replicon in OR6 cells. Specific inhibition of the replication of a full-length HCV genotype 1b replicon by (a) IFN-α and (b) IFN-λ1, (c) IFN-λ2, (d) IFN-λ3 were quantified on the basis of luciferase activity. Symbols show the mean value of triplicate wells; error bars show the SD. *: $P < 0.05$ *vs* control (IFN 0 ng/mL) of each time point.

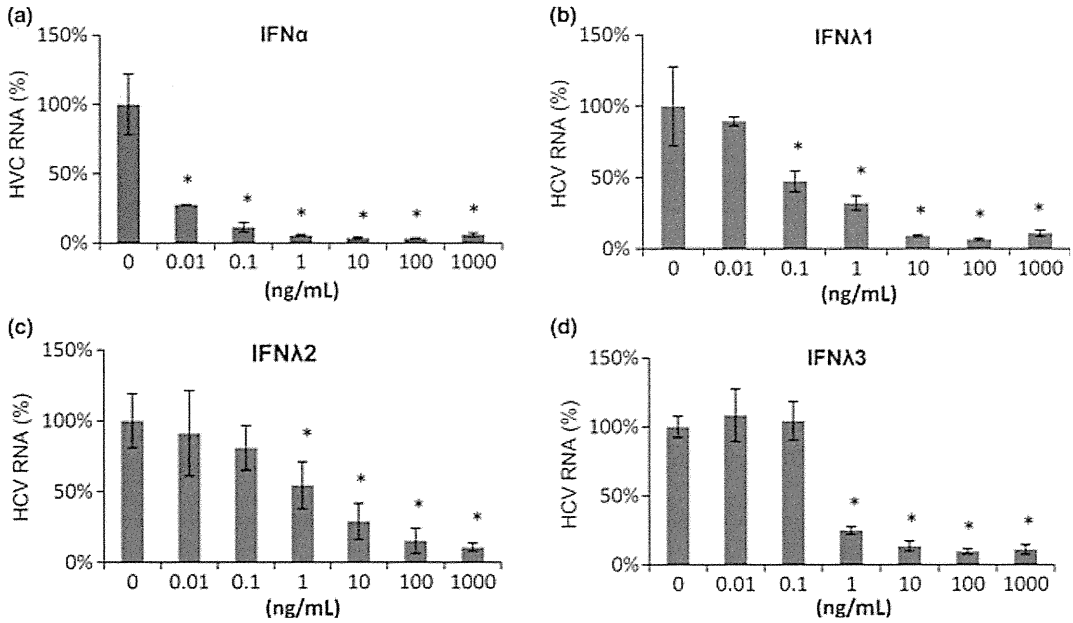

Fig. 2 IFN-α and IFN-λs inhibit HCV replicon in Huh7.5.1 cells. JFH1-infected Huh7.5.1 cells were incubated with various concentrations of (a) IFN-α and (b) IFN-λ1, (c) IFN-λ2, (d) IFN-λ3. After 48 h of treatment, total RNA was isolated and reverse transcribed, after which quantitative PCR was performed. Symbols show the mean value of triplicate wells; error bars show the SD. *: $P < 0.05$ *vs* control (IFN 0 ng/mL).

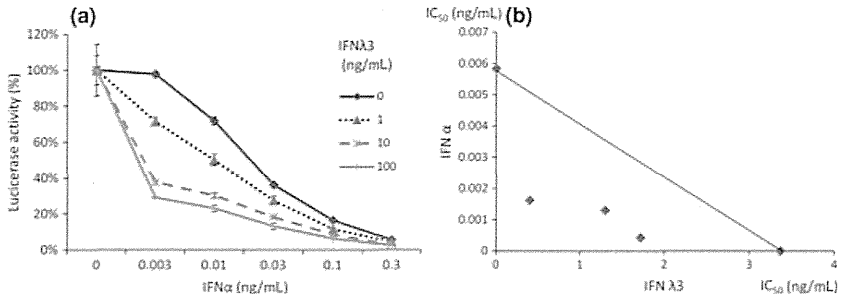

Fig. 3 Synergistic inhibitory effect of IFN-λ3 with IFN-α on hepatitis C virus replication. OR6/ORN/C-5B/KE cells were treated with combinations of IFN-λ3 with IFN-α at various concentrations. (a) The relative concentration–inhibition curves of IFN-α plotted for each fixed concentration of IFN-λ3 (0, 1, 10 and 100 ng/mL). (b) Classic isobologram for IC_{50} of IFN-λ3 with IFN-α in combination.

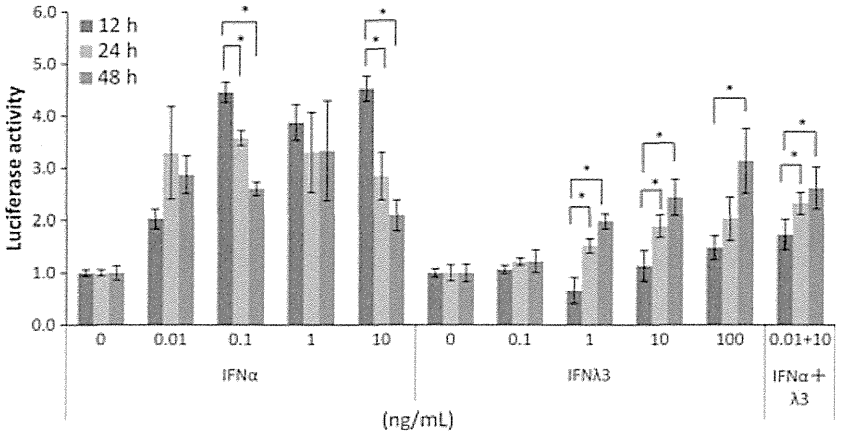

Fig. 4 IFN-stimulated response element (ISRE) promoter activity induced by IFN-α, IFN-λ3 or combination of IFN-α and IFN-λ3. OR6/ORN/C-5B/KE cells transfected with ISRE-firefly luciferase were cultured with various concentrations of IFN-α alone, IFN-λ3 alone or 0.01 ng/mL IFN-α plus 10 ng/mL IFN-λ3. ISRE-firefly luciferase activity at 24 h after transfection. Symbols show the mean value of triplicate wells; error bars show the SD. *: $P < 0.05$.

At all time points, the IFN-λ3-treated samples showed a tendency for the induction of a larger number of genes than samples treated with IFN-α. However, as shown in Table 1 listing the top 25 genes that were upregulated by both IFN-α and IFN-λ3 at 12 h, most of the upregulated genes are previously identified ISGs and the genes with high ranks were similar irrespective of the type of IFN or time point.

The time course of ISGs regulation differs between IFN-α and IFN-λ3

By microarray analysis, ISGs were more rapidly induced after the addition of IFN-α *vs* IFN-λ3 (data not shown). To confirm the rapid induction of ISGs by IFN-α, six ISGs, that is, IFI-6, IFIT1 (ISG56), DDX60, OAS2, Mx1 and USP18, were quantified for time-dependent expressional change by real-time RT-PCR. Expression of most of the genes upregulated by IFN-α peaked at 12 h and fell thereafter. In contrast, expression of IFN-λ3-induced genes peaked at 24 h and lasted up to 48 h. Combination of IFN-α and IFN-λ3 induced ISG with peak effects occurring at 12–24 h and lasting up to 48 h (Fig. 5).

DISCUSSION

In this study, we demonstrated that IFN-λ family members have distinctive time-dependent antiviral activities in an HCV replicon system and that IFN-λ3 and IFN-α have a synergistic effect in combination. Moreover, we attempted to identify the antiviral mechanism of IFN-λ3 by conducting a cDNA microarray analysis.

In previous studies, anti-HCV activity of IFN-λ1, IFN-λ2 and IFN-λ3 was reported in JFH-1 and OR6/C-5B systems [13]. Time-dependent anti-HCV activity has also been observed with IFN-λ1 [9]. In this study, we confirmed the previous results and added the further finding that time-dependent antiviral activity is not limited to IFN-λ1, but rather is common among all IFN-λs.

Table 1 Top 25 genes that were upregulated by both IFN-α and IFN-λ3 at 12 h

Gene bank ID	Gene symbol	Gene description	IFN-α 0.01 ng/mL fold increase	IFN-λ3 10 ng/mL fold increase	IFN-α+IFN-λ3 fold increase
BC007091	IFIT1	Interferon-induced protein with tetratricopeptide repeats 1	4.01	4.49	4.87
BC049215	OAS2	2′-5′-oligoadenylate synthetase 2, 69/71kDa	3.06	3.88	4.48
M33882	MX1	Myxovirus (influenza virus) resistance 1	3.24	3.29	3.69
AF095844	IFIH1	Interferon induced with helicase C domain 1	2.73	3.02	3.54
BC038115	DDX60	DEAD (Asp-Glu-Ala-Asp) box polypeptide 60	2.70	2.92	3.51
BC011601	IFI6	Interferon, alpha-inducible protein 6	3.07	3.24	3.42
BC042047	HERC6	Hect domain and RLD 6	2.56	2.75	3.34
AF442151	RSAD2	Radical S-adenosyl methionine domain containing 2	1.32	2.59	3.28
U34605	IFIT5	Interferon-induced protein with tetratricopeptide repeats 5	2.47	2.91	3.25
AY730627	OAS1	2′,5′-oligoadenylate synthetase 1, 40/46kDa	2.32	2.57	3.05
AB006746	PLSCR1	Phospholipid scramblase 1	2.37	2.51	3.03
AF307338	PARP9	Poly (ADP-ribose) polymerase family, member 9	2.39	2.46	2.94
M87503	IRF9	Interferon regulatory factor 9	2.61	2.59	2.85
AK297137	IFIT3	Interferon-induced protein with tetratricopeptide repeats 3	1.90	2.36	2.79
AK290655	EIF2AK2	Eukaryotic translation initiation factor 2-alpha kinase 2	2.47	2.45	2.77
BX648758	PARP14	Poly (ADP-ribose) polymerase family, member 14	2.07	2.25	2.66
BC132786	DDX58	DEAD (Asp-Glu-Ala-Asp) box polypeptide 58	1.83	2.17	2.59
AF445355	SAMD9	Sterile alpha motif domain containing 9	2.07	2.08	2.56
	DDX60L	DEAD (Asp-Glu-Ala-Asp) box polypeptide 60-like	1.63	1.92	2.39
BC014896	USP18| USP41	Ubiquitin-specific peptidase 18/ubiquitin-specific peptidase 41	1.52	1.78	2.11
AB044545	OAS3	2′-5′-oligoadenylate synthetase 3, 100kDa	1.44	1.57	2.10
BC010954	CXCL10	Chemokine (C-X-C motif) ligand 10	0.76	1.66	1.99
BC014896	USP18	Ubiquitin-specific peptidase 18	1.33	1.55	1.99
AL832618	IFI44L	Interferon-induced protein 44-like	0.58	1.31	1.95

We also assessed whether IFN-λ3 and IFN-α in combination could produce additive or synergistic effects on antiviral activity. In previous studies, additive antiviral activity against HCV was reported with the combination of IFN-λ1 and IFN-α [9, 10]. However, there have been no previous reports on the combined effects of IFN-λ3 and IFN-α. In this study, the focus was on IFN-λ3, because IFN-λ3 is suspected to be the key molecule, mediating the effect of SNPs in the IL-28B gene region on the anti-HCV response to IFN-α. As shown in Fig. 3 and Table S1, synergistic induction of anti-HCV activity occurred in both the OR6/C-5B and Huh7.5/JFH-1 HCV replicon systems. Synergy was demonstrated by the combination index values (Table S1).

Although it has been reported that the upregulated genes induced by IFN-λ are similar to those induced by IFN-α [9, 14–16], there have been no previous reports on

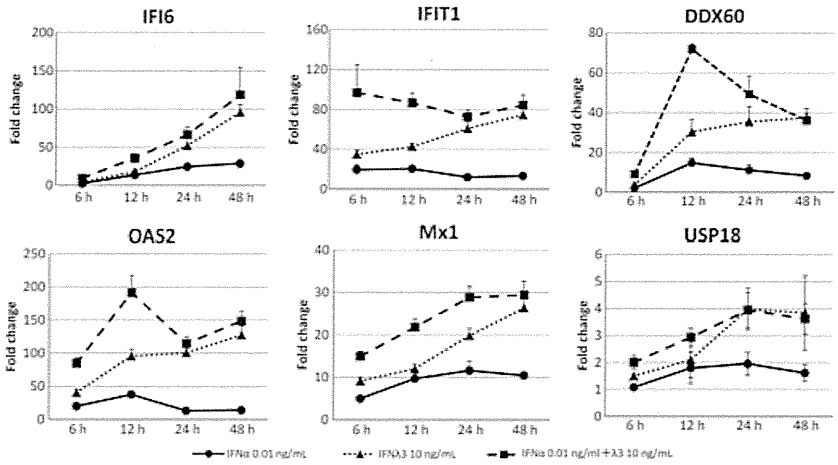

Fig. 5 Time course of ISG expression induced by 0.01 ng/mL IFN-α, 10 ng/mL IFN-λ3 or 0.01 ng/mL IFN-α plus 10 ng/mL IFN-λ3. Expression of the ISGs – IFI-6, IFIT1 (ISG56), DDX60, OAS2, Mx1 and USP18 – in OR6/ORN/C-5B/KE cells treated 6, 12, 24 and 48 h were determined by qRT-PCR. Results are presented as the relative fold induction. Symbols show the mean value of triplicate wells; error bars show the SD. *Solid lines* represent 0.01 ng/mL IFN-α alone, whereas *fine dashed lines* show 10 ng/mL IFN-λ3 alone, and *coarse dashed lines* show the combination of the 2 cytokines.

the genes induced by IFN-α and IFN-λ in combination. In cDNA microarray analysis, as demonstrated in Table 1, the most strongly upregulated genes induced by IFN-α/IFN-λ3 alone or in combination were almost identical, and most of them were ISGs. As no genes showed upregulation specific to IFN-λ3, we speculate that IFN-α and IFN-λ3 share a similar antiviral intracellular mechanism at the molecular level.

Unexpectedly in microarray analyses, synergistic upregulation of ISGs was not observed. In the same manner, TaqMan real-time RT-PCR analysis showed that the combination of IFN-α and IFN-λ3 did not upregulate ISGs synergistically (Fig. 5). In addition to cDNA microarray analysis, ISRE reporter assays were performed to determine the activation of components of the JAK-STAT pathway common to both type I and III IFNs. As shown in Fig. 4, each IFN upregulated ISRE activity, and the combination of IFN-λ3 and IFN-α did not synergistically enhance ISRE activity either.

Meanwhile, the peak time of the induction of ISG expression differs for IFN-α and IFN-λ1 [9, 17]; peak gene expression occurs earlier with IFN-α than with IFN-λ1. In our study, we confirmed that the peak induction of gene expression occurred later (24 h) and lasted longer (24–48 h) with IFN-λ3 than with IFN-α (12 h). Importantly, gene expression appeared early (12 h) and was prolonged (48 h) by the combination of both IFNs. Similarly to the peak time difference between IFN-α and IFN-λ3 seem for ISG expression, a time-dependent increase in ISRE activation was observed with the combination of both IFNs. While the precise mechanism remains to be clarified, differential regulation of the time-dependent induction of ISG gene expression could be one of the mechanisms underlying the synergistic antiviral effect. One of the molecules contributing to time-dependent ISG upregulation is the ISG known as ubiquitin-specific peptidase 18 (USP18), which has been reported to bind to IFNAR2 and inhibit the interaction of Jak1 with its receptor, thereby preventing IFN-α signalling while leaving IFN-λ signalling unaffected [18, 19]. Actually, expression of USP18 is specifically upregulated with IFN-λ3 in this study as shown in Fig. 5. If the ISGs upregulated by IFN-α are downregulated by USP18, it is plausible that the expression of genes induced by IFN-α decreases early, while expression of genes induced by IFN-λ lasts longer.

A number of clinical studies have confirmed that SNPs around the IL-28B gene are associated with the response to PEG-IFN and RBV therapy, and as previously indicated, various investigations have been performed to clarify the underlying mechanism. Specifically, increased IL-28B mRNA expression in PBMC [2, 3], high serum concentrations of IFN-λ1 (IL-29) [20], low expression of ISGs in the liver prior to IFN treatment [8, 21] and high upregulation of ISG expression by IFN treatment [8, 22] were found in subjects with IL-28B SNP genotypes associated with SVR (rs12979860 CC and rs8099917 TT). Although the functional role of IFN-λ3 still needs to be investigated more thoroughly, if IFN-λ3 expression change is the essential difference in determining the clinical treatment response to PEG-IFN and RBV therapy and if its expression is decreased in patients with the specific IL-28B genotype, which is associated with non-SVR, it is possible that exogenous administration of IFN-λ3 might improve IFN-α-induced viral clearance and that such treatment would be beneficial for patients with the IFN-resistant IL-28B genotype.

In present study, the OR6-cultured cells harboured the rs8099917 TT genotype, and recombinant IFN-λ3 (IL-

28B) protein used in the experiment was derived from cells with the rs8099917 TT genotype (data not shown). Therefore, the viral responses and/or cellular gene expression change in cells and/or proteins with different IL-28B genotypes *in vitro* should be determined in future studies.

In conclusion, we demonstrated that IFN-α and IFN-λ3 synergistically enhance anti-HCV activity *in vitro*. Although the ISGs upregulated by IFN-α and IFN-λ3 were similar, differences in time-dependent upregulation of these genes, especially prolonged ISGs expression by IFN-λ3, might contribute to their synergistic antiviral activity.

ACKNOWLEDGEMENTS

We are grateful to Ms. Sakamoto, Ms. Endo and Mr. Osada, laboratory technicians at University of Yamanashi Hospital, for quantification of HCV core protein in culture supernatant. This study was supported in part by a grant-in-aid scientific research fund of the Ministry of Education, Science, Sports and Culture number 21590836, 21590837, 23390195 and in part by a grant-in-aid from the Ministry of Health, Labour and Welfare of Japan (H22-kanen-006).

CONFLICT OF INTEREST

Shinya Maekawa and Taisuke Inoue belong to a donation-funded department that is funded by MSD co. ltd.

REFERENCES

1 Ge D, Fellay J, Thompson AJ, *et al.* Genetic variation in IL28B predicts hepatitis C treatment-induced viral clearance. *Nature* 2009; 461: 399–401.
2 Tanaka Y, Nishida N, Sugiyama M, *et al.* Genome-wide association of IL28B with response to pegylated interferon-alpha and ribavirin therapy for chronic hepatitis C. *Nat Genet* 2009; 41: 1105–1109.
3 Suppiah V, Moldovan M, Ahlenstiel G, *et al.* IL28B is associated with response to chronic hepatitis C interferon-alpha and ribavirin therapy. *Nat Genet* 2009; 41: 1100–1104.
4 Thomas DL, Thio CL, Martin MP, *et al.* Genetic variation in IL28B and spontaneous clearance of hepatitis C virus. *Nature* 2009; 461: 798–801.
5 Rauch A, Kutalik Z, Descombes P, *et al.* Genetic variation in IL28B is associated with chronic hepatitis C and treatment failure: a genome-wide association study. *Gastroenterology* 2010; 138:1338–1345, 1345 e1331-1337.
6 Dellgren C, Gad HH, Hamming OJ, Melchjorsen J, Hartmann R. Human interferon-lambda3 is a potent member of the type III interferon family. *Genes Immun* 2009; 10: 125–131.
7 Kotenko SV, Gallagher G, Baurin VV, *et al.* IFN-lambdas mediate antiviral protection through a distinct class II cytokine receptor complex. *Nat Immunol* 2003; 4: 69–77.
8 Honda M, Sakai A, Yamashita T, *et al.* Hepatic ISG expression is associated with genetic variation in interleukin 28B and the outcome of IFN therapy for chronic hepatitis C. *Gastroenterology* 2010; 139: 499–509.
9 Marcello T, Grakoui A, Barba-Spaeth G, *et al.* Interferons alpha and lambda inhibit hepatitis C virus replication with distinct signal transduction and gene regulation kinetics. *Gastroenterology* 2006; 131: 1887–1898.
10 Pagliaccetti NE, Eduardo R, Kleinstein SH, Mu XJ, Bandi P, Robek MD. Interleukin-29 functions cooperatively with interferon to induce antiviral gene expression and inhibit hepatitis C virus replication. *J Biol Chem* 2008; 283: 30079–30089.
11 Ikeda M, Abe K, Dansako H, Nakamura T, Naka K, Kato N. Efficient replication of a full-length hepatitis C virus genome, strain O, in cell culture, and development of a luciferase reporter system. *Biochem Biophys Res Commun* 2005; 329: 1350–1359.
12 Aoyagi K, Ohue C, Iida K, *et al.* Development of a simple and highly sensitive enzyme immunoassay for hepatitis C virus core antigen. *J Clin Microbiol* 1999; 37: 1802–1808.
13 Zhang L, Jilg N, Shao RX, *et al.* IL28B inhibits hepatitis C virus replication through the JAK-STAT pathway. *J Hepatol* 2011; 55: 289–298.
14 Ank N, West H, Bartholdy C, Eriksson K, Thomsen AR, Paludan SR. Lambda interferon (IFN-lambda), a type III IFN, is induced by viruses and IFNs and displays potent antiviral activity against select virus infections in vivo. *J Virol* 2006; 80: 4501–4509.
15 Zhou Z, Hamming OJ, Ank N, Paludan SR, Nielsen AL, Hartmann R. Type III interferon (IFN) induces a type I IFN-like response in a restricted subset of cells through signaling pathways involving both the Jak-STAT pathway and the mitogen-activated protein kinases. *J Virol* 2007; 81: 7749–7758.
16 Doyle SE, Schreckhise H, Khuu-Duong K, *et al.* Interleukin-29 uses a type 1 interferon-like program to promote antiviral responses in human hepatocytes. *Hepatology* 2006; 44: 896–906.
17 Maher SG, Sheikh F, Scarzello AJ, *et al.* IFNalpha and IFNlambda differ in their antiproliferative effects and duration of JAK/STAT signaling activity. *Cancer Biol Ther* 2008; 7: 1109–1115.
18 Makowska Z, Duong FH, Trincucci G, Tough DF, Heim MH. Interferon-beta and interferon-lambda signaling is not affected by interferon-induced refractoriness to interferon-alpha in vivo. *Hepatology* 2011; 53: 1154–1163.
19 Franois-Newton V, de Freitas Almeida GM, Payelle-Brogard B, *et al.*

USP18-Based Negative Feedback Control Is Induced by Type I and Type III Interferons and Specifically Inactivates Interferon α Response. *PLoS ONE* 2011; 6: e22200.
20 Langhans B, Kupfer B, Braunschweiger I, *et al.* Interferon-lambda serum levels in hepatitis C. *J Hepatol* 2011; 54: 859–865.
21 Urban TJ, Thompson AJ, Bradrick SS, *et al.* IL28B genotype is associated with differential expression of intrahepatic interferon-stimulated genes in patients with chronic hepatitis C. *Hepatology* 2010; 52: 1888–1896.
22 Abe H, Hayes CN, Ochi H, *et al.* IL28 variation affects expression of interferon stimulated genes and peg-interferon and ribavirin therapy. *J Hepatol* 2011; 54: 1094–1101.

SUPPORTING INFORMATION

Additional Supporting Information may be found in the online version of this article:

Figure S1: IFN-α and IFN-λs inhibit HCV core protein secretion. JFH1-infected Huh7.5.1 cells were incubated with various concentrations of IFN-α and IFN-λ1, -λ2, -λ3. After 48 h of treatment, HCV core protein in the medium was measured. Symbols show the mean value of triplicate wells; error bars show the SD. *: $p < 0.05$ vs. control (IFN 0ng/ml).

Figure S2: The dimethylthiazol carboxymethoxyphenyl sulfophenyl tetrazolium assay was performed after OR6/ORN/C-5B/KE cells were cultured with various concentrations of (A) IFN-α, (B) IFN-λ1, (C) IFN-λ2, (D) IFN-λ3 and (E) combination of IFN-α and IFN-λ3 for 48 h. Symbols show the mean value of triplicate wells; error bars show the SD. *: $p < 0.05$ vs. control (IFN 0ng/ml).

Figure S3: The dimethylthiazol carboxymethoxyphenyl sulfophenyl tetrazolium assay was performed after Huh7.5.1/JFH-1 cells were cultured with various concentrations of (A) IFN-α, (B) IFN-λ1, (C) IFN-λ2, (D) IFN-λ3 and (E) combination of IFN-α and IFN-λ3 for 48 h. Symbols show the mean value of triplicate wells; error bars show the SD. *: $p < 0.05$ vs. control (IFN 0ng/ml).

Table S1: Combination index after 48hr stimulation by CalucSyn.

Please note: Wiley-Blackwell are not responsible for the content or functionality of any supporting materials supplied by the authors. Any queries (other than missing material) should be directed to the corresponding author for the article.

J Gastroenterol (2014) 49:163–164
DOI 10.1007/s00535-013-0926-7

EDITORIAL

Once-daily simeprevir in combination with pegylated-interferon and ribavirin: a new horizon in the era of direct-acting antiviral agent therapy for chronic hepatitis C

Shinya Maekawa · Nobuyuki Enomoto

Received: 7 December 2013 / Accepted: 10 December 2013 / Published online: 21 December 2013

Hepatitis C virus (HCV) is a leading cause of chronic hepatitis, liver cirrhosis, and hepatocellular carcinoma (HCC), and it is estimated that infected individuals total 185 million people worldwide. In Japan, around 2 million are infected with HCV, and more than 20 thousand die from HCV-induced HCC annually. Though viral eradication with antiviral therapies is the most important and effective choice for decreasing HCC-related deaths induced by HCV, complete viral eradication has been quite difficult till recently, especially in patients with genotype-1 HCV infection because of the low response rate to interferon (IFN)-based therapy [1, 2].

In this background, development of novel direct-acting antiviral agents (DAAs) specific for HCV was truly a revolutionary event. In 2011, two first-generation NS3 protease inhibitors (PIs), telaprevir and boceprevir, were firstly approved among all the DAAs for clinical use in USA and Europe for genotype-1 HCV in combination with pegylated-interferon and ribavirin (PR), while telaprevir was approved in Japan in the same 2011 period. As expected, a regimen including telaprevir in combination with pegylated-interferon and ribavirin dramatically improved the sustained viral response (SVR) rate to as high as 80 % in genotype-1 HCV infection. On the other hand, telaprevir has several undesirable problems. Among all, adverse events (AEs) of anemia and skin rash are serious problems of telaprevir, and Grade 3/4 skin disorders, including Stevens–Johnson syndrome and drug rashes with eosinophilia and systemic symptoms, as well as Grade 3 anemia (<8.0 g/dL), might occur [3, 4]. Moreover, cumbersome frequent dosing three times a day (every 7–9 h) could induce poor medication adherence. Under the circumstances, it has been quite stressful for patients as well as clinicians to introduce and monitor this telaprevir-based regimen.

Simeprevir (SMV, TMC435) is classified as a second-generation PI with the macrocyclic structure having an advantage in the binding affinity and specificity for NS3 protease compared to the first-generation PI with the linear structure. Due to the difference in the structure, the drug-resistance profile is somewhat different from that of telaprevir. Though simeprevir shows cross-resistance with telaprevir at amino acid positions of 155 and 156, most of the resistant mutation occurs at the simeprevir-specific amino acid position of 168 [5]. Though simeprevir is effective in all viral genotypes (genotype 1–6), it has the strongest antiviral activity for genotype-1a and -1b HCV infection. In particular, low AE rate and its patient-friendly once-daily dosing are the important characters of simeprevir aside from its strong antiviral activity. In the international phase II trials of simeprevir in combination with PegIFNa-2a/RBV for treatment-naïve (PILLAR study) [6] and treatment-experienced patients (ASPIRE study) [7] for HCV genotype 1-infected patients, it was demonstrated that simeprevir was generally well tolerated and had a pharmacokinetic profile supporting once-a-day (QD) dosing resulting in high virologic response rates.

In this issue of the *Journal of Gastroenterology*, Hayashi et al. [8] reported the important results of the phase II *D*ose and duration *R*anging study of *A*ntiviral agent TMC435 in *G*enotype *O*ne HCV treatment-*N*aïve patients (DRAGON study; TMC435-C215) evaluating once-daily simeprevir

This comment refers to the article available at doi:10.1007/s00535-013-0875-1.

S. Maekawa (✉) · N. Enomoto
First Department of Internal Medicine, Faculty of Medicine, University of Yamanashi, 1110 Shimokato, Chuo, Yamanashi 409-3898, Japan
e-mail: maekawa@yamanashi.ac.jp

with pegylated-interferon and ribavirin therapy for treatment-naïve, high viral-loaded hepatitis C genotype 1-infected patients in Japan. Due to the result of previous phase I study that simeprevir plasma concentration was higher in Japanese healthy volunteers compared with Caucasian volunteers, simeprevir doses of 50/100 mg QD were selected for this study, while simeprevir doses of 150 mg QD were selected in western countries [9]. Through investigating five treatment groups (SMV12/PR24 50 mg, SMV12/PR24 100 mg, SMV24/PR24 50 mg, SMV24/PR24 100 mg, and PR48), it was disclosed that simeprevir-combined groups all achieved high SVR rate (77–92 % compared to 46 % for PR). As to the AEs, simeprevir was well tolerated, and the incidence of anemia and skin rash were similar in their frequency and their grade between all the SMV groups and the PR group. Due to low AEs, therapy discontinuation rate and ribavirin dose reduction was also similar in the SMV groups and the PR group. While an AE of bilirubin elevation was specific to simeprevir, and it reached to grade 3 (2.6–5.0 mg/dL) to 4 (>5.0 mg/dL) in four patients (5 %) leading to the discontinuation of simeprevir in these individuals, the bilirubin level returned to baseline after the end of simeprevir in those patients. Since bilirubin elevation is considered to result from the blockade of bilirubin clearance-associated OATP1B1 and MRP transporters by simeprevir [10], it is considered that the bilirubin elevation by simeprevir does not reflect deterioration of liver function.

Following the results of this phase II DRAGON study, treatment dosage of simeprevir was determined as 100 mg QD in Japan, and successive phase III CONCERTO studies for simeprevir/pegylated-interferon/ribavirin therapy have been conducted (CONCERTO-1 for treatment-naïve, -2 for previous null responder, -3 for previous relapser, and -4 for naïve, null responder and relapser). After the completion of those CONCERTO studies with favorable outcomes for simeprevir-based regimens, once-daily simeprevir with pegylated-interferon and ribavirin therapy for high viral-loaded hepatitis C genotype 1-infected patients was just recently approved for clinical use in Japan.

Considering the history of HCV therapy, this new therapy of once-daily simeprevir with pegylated-interferon and ribavirin therapy is ideal in its high efficacy and low AEs. Of course, it is true that DAA combination therapies without IFN (IFN-free therapies) would appear in the near future, and that these IFN-free therapies are advantageous in that they are free from IFN-related AEs. However, in terms of DAA-resistant viral mutants, it is considered that these mutant HCVs generally have low replication fitness, and are sensitive to IFN. Therefore, it is speculated that IFN-based DAA therapies compared to IFN-free DAA therapies are safer in preventing the development of multidrug resistant HCVs.

Taken together, the new regimen of once-daily simeprevir with pegylated-interferon and ribavirin therapy would surely be an important milestone in the therapy for high viral-loaded hepatitis C genotype-1 infected patients in the era of DAA therapy.

References

1. Kim MN, Kim BK, Han KH. Hepatocellular carcinoma in patients with chronic hepatitis C virus infection in the Asia-Pacific region. J Gastroenterol. 2013;48(6):681–8.
2. Thomas DL. Global control of hepatitis C: where challenge meets opportunity. Nat Med. 2013;19(7):850–8.
3. Chayama K, Hayes CN, Ohishi W, Kawakami Y. Treatment of chronic hepatitis C virus infection in Japan: update on therapy and guidelines. J Gastroenterol. 2013;48(1):1–12.
4. Kumada H, Toyota J, Okanoue T, Chayama K, Tsubouchi H, Hayashi N. Telaprevir with peginterferon and ribavirin for treatment-naive patients chronically infected with HCV of genotype 1 in Japan. J Hepatol. 2013;56(1):78–84.
5. Lenz O, Verbinnen T, Lin TI, Vijgen L, Cummings MD, Lindberg J, et al. In vitro resistance profile of the hepatitis C virus NS3/4A protease inhibitor TMC435. Antimicrob Agents Chemother. 2010;54(5):1878–87.
6. Fried MW, Buti M, Dore GJ, Flisiak R, Ferenci P, Jacobson I, et al. Once-daily simeprevir (TMC435) with pegylated interferon and ribavirin in treatment-naive genotype 1 hepatitis C: the randomized PILLAR study. Hepatology. 2013;58(6):1918–29.
7. Zeuzem S, Berg T, Gane E, Ferenci P, Foster GR, Fried MW, et al. Simeprevir increases rate of sustained virologic response among treatment-experienced patients with HCV genotype-1 infection: a phase IIb trial. Gastroenterology. 2013. doi:10.1053/j.gastro.2013.10.058.
8. Hayashi N, Seto C, Kato M, Komada Y, Goto S. Once-daily simeprevir (TMC435) with peginterferon/ribavirin for treatment-naïve hepatitis C genotype 1-infected patients in Japan: the DRAGON study. J Gastroenterol. 2013. doi:10.1007/s00535-013-0875-1.
9. Verloes R, Shishido A. Phase I safety and PK of TMC435 in healthy volunteers and safety, PK and short-term efficacy in chronic hepatitis C infected individuals. Kobe: Abstract O-32 presented at the Japanese Hepatology Congress; 2009. p. 4–5.
10. Huisman MT, Snoeys J, Monbaliu J, Martens M, Sekar V, Raoof A. In vitro studies investigating the mechanism of interaction between TMC435 and hepatic transporters. Poster 278 presented at the 61st Annual Meeting of the American Association for the Study of Liver Diseases (AASLD), Boston, USA, October 29–November 2, 2010.

Hepatocellular carcinoma risk assessment using gadoxetic acid-enhanced hepatocyte phase magnetic resonance imaging

Nobutoshi Komatsu[1)], Utaroh Motosugi[2)], Shinya Maekawa[1)], Kuniaki Shindo[1)], Minoru Sakamoto[1)], Mitsuaki Sato[1)], Akihisa Tatsumi[1)], Mika Miura[1)], Fumitake Amemiya[1)], Yasuhiro Nakayama[1)], Taisuke Inoue[1)], Mitsuharu Fukasawa[1)], Tomoyoshi Uetake[1)], Masahiko Ohtaka[1)], Tadashi Sato[1)],Yasuhiro Asahina[3)], Masayuki Kurosaki[4)], Namiki Izumi[4)], Tomoaki Ichikawa[2)], Tsutomu Araki[2)] and Nobuyuki Enomoto[1)]

1) First Department of Internal Medicine, University of Yamanashi
1110, Shimokato, Chuo-shi, Yamanashi, Japan 409-3898
2) Department of Radiology, University of Yamanashi
1110, Shimokato, Chuo-shi, Yamanashi, Japan 409-3898
3) Department of Gastroenterology and Hepatology, Tokyo Medical and Dental University
1-5-45 Yushima, Bunkyo-ku, Tokyo, Japan 113-8510
4) Department of Gastroenterology and Hepatology, Musashino Red Cross Hospital,
1-26-1 Kyonan-cho, Musashino-shi, Tokyo, Japan 180-8610

Short running title: HCC risk assessment using EOB-enhanced MRI

This article has been accepted for publication and undergone full peer review but has not been through the copyediting, typesetting, pagination and proofreading process, which may lead to differences between this version and the Version of Record. Please cite this article as doi: 10.1111/hepr.12309

Keywords: hepatocellular carcinoma, magnetic resonance imaging, gadoxetic acid, hepatocyte phase, risk assessment

FOOTNOTES

Competing interests

All authors have no conflict of interest related to this manuscript.

Funding

This study was supported in part by a grant-in-aid from the Ministry of Education, Science, Sports and Culture of Japan (23390195, 23791404, 24590964 and 24590965), and in part by a grant-in-aid from the Ministry of Health, Labour, and Welfare of Japan (H23-kanen-001, H23-kanen-004, H23-kanen-006, H24-kanen-002, H24-kanen-004 and H25-kanen-006).

Correspondence:

Nobuyuki Enomoto, M.D. / Ph.D.

First Department of Internal Medicine,University of Yamanashi,

1110, Shimokato, Chuo, Yamanashi, 409-3898, Japan.

Tel: +81-55-273-9584

Fax: +81-55-273-6748

E-mail: enomoto@yamanashi.ac.jp

List of Abbreviations

HCC: Hepatocellular Carcinoma

MRI: Magnetic Resonance Imaging

US: Ultrasonography

CT: Computed Tomography

HBV: Hepatitis B Virus

HCV: Hepatitis C Virus

AASLD: American Association for the Study of Liver Diseases

T1WIs: T1-Weighted Images

T2WIs: T2-Weighted Images

ALT: Alanine Aminotransferase

γ-GTP: γ - Glutamyl Transpeptidase

AFP: Alpha-fetoprotein

HR: Hazard Ratio

CI: Confidence Interval

DWIs: Diffusion-Weighted Images

ABSTRACT

Aim: To investigate whether the patients with hypovascular liver nodules determined on the arterial phase and hypointensity on the hepatocyte phase gadoxetic acid-enhanced magnetic resonance imaging (hypovascular hypointense nodules) are at increased risk of hepatocarcinogenesis, we assessed subsequent typical hepatocellular carcinoma (HCC) development at any sites of the liver with and without such nodules.

Methods: One hundred and twenty-seven patients with chronic hepatitis B or C and without a history of HCC, including 68 with liver cirrhosis, were divided into those with (non-clean liver group, n = 18) and without (clean liver group, n =109) hypovascular hypointense nodules. All the patients were followed-up for 3 years, and HCC development rates and risk factors were analyzed with the Kaplan-Meier method and the Cox proportional hazard model, respectively.

Results: A total of 17 patients (10 in the non-clean liver group and 7 in the clean liver group) developed typical HCCs. Cumulative 3-year rates of HCC development were 55.5% in the non-clean liver group and 6.4% in the clean liver group ($p < 0.001$), and those at the different sites from the initial nodules was also higher in the non-clean liver group (22.2%) than the clean liver group (6.4%) ($p=0.003$). Multivariate analysis identified older age ($p = 0.024$), low platelet counts ($p = 0.017$) and a non-clean liver ($p < 0.001$) as independent risk factors for subsequent HCC development.

Conclusions: Patients with hypovascular hypointense liver nodules are at a higher risk for HCC development at any sites of the liver than those without such nodules.

INTRODUCTION

Hepatocellular carcinoma (HCC) is one of the most common cancers worldwide and is a major cause of death in patients with chronic viral liver disease. Despite many advances in multidisciplinary treatment, complete curative treatment of early-stage HCC remains the only possible therapeutic choice for long-term survival. Therefore, surveillance programs for patients at a high-risk for HCC that include imaging-based evaluations are crucial for the detection and treatment of early-stage HCC.

The newly introduced magnetic resonance imaging (MRI) contrast agent, gadolinium ethoxybenzyl diethylenetriaminepentaacetic acid (gadoxetic acid), has enabled concurrent assessment of tumor vascularity and unique hepatocyte-specific contrast (hepatocyte phase) (1-3). This has led to the frequent identification of hypovascular nodules determined on the arterial phase with hypointensity on the hepatocyte phase (hypovascular hypointense nodules) (4-8), while many of these nodules are difficult to be detected by ultrasonography (US) or computed tomography (CT). Recently, the natural history of hypovascular hypointense nodules themselves were reported in several studies (9-12), revealing the high risk of subsequent progress to typical HCCs from these nodules. However, it is not well known whether patients with such nodules has a higher risk of developing typical HCCs at any sites of the liver, including at the different sites from initial nodules, compared to those without such nodules.

If patients with these nodules may have a high risk of developing typical HCCs not only at the same sites but also at the different sites from initial nodules, significant proportion of these nodules are precancerous lesions or early-stage HCC as reported

(13-15), and more importantly, the liver with these nodules might reflect a higher potential for hepato-carcinogenesis or the presence of undetectable precursor lesions in other sites of the liver. Conversely, the absence of these nodules potentially identifies the patients at a low risk for subsequent typical HCC development at any sites. The purpose of this study was to assess the risk of subsequent typical HCC development at any sites of the liver with and without hypovascular hypointense nodules on gadoxetic acid–enhanced MRI.

METHODS

Ethical review

The protocol of this retrospective study was approved by the ethics committee of Yamanashi University Hospital, which waived the requirement for written informed consent because the study was a retrospective data analysis, with appropriate consideration given to patient risk, privacy, welfare, and rights.

Patients

We recruited 559 consecutive outpatients with chronic hepatitis B virus (HBV) or hepatitis C virus (HCV) infection who underwent gadoxetic acid-enhanced MRI at Yamanashi University Hospital between January 2008 and December 2010. The exclusion criteria were as follows: 1) presence or history of typical HCC (n = 420), because intrahepatic metastasis does not always develop through the usual multistep hepatocarcinogenesis process, skipping the early pathological stage with hypovascularity to an advanced pathological stage even when the size is small (16, 17); 2) Child-Pugh class C disease (n = 9), because the hepatocyte phase findings are not reliable in patients with this condition because of reduced gadoxetic acid uptake in the liver (18); and 3) patients who dropped out during the 3-year follow-up period (n = 3).

After excluding 432 patients, 127 patients were included in this retrospective cohort study. They were divided into groups with hypovascular nodules determined on the arterial phase and hypointensity on the hepatocyte phase (non-clean liver group; n = 18 patients) and without such nodules (clean liver group; n = 109 patients) as shown in Figure 1. In this study, we divided cases into two groups according to the presence or

absence of these nodules at the baseline, even when such nodules were initially detected during the follow-up period; we assigned these patients to the clean liver group.

Follow-up and diagnosis of HCC

All 127 patients were followed-up at the liver disease outpatient clinic of our institution with blood tests, including those for tumor markers, and diagnostic imaging modality (US, CT or MRI). The development of typical HCC that required treatment as proposed by the American Association for the Study of Liver Diseases (AASLD) guidelines (19) and that was diagnosed according to imaging criteria, showing arterial hypervascularity and venous phase washout, or based on histological examination of liver biopsies from hypovascular nodules that grew to >10 mm during follow-up. Biopsies were obtained using a 21-gauge core needle. Two patients each had a liver nodule >10 mm in diameter on initial MRI (12mm and 13mm), was diagnosed on the basis of the biopsy as a dysplastic nodule.

The endpoint of this study was the development of typical HCC not only from the hypovascular hypointense nodules observed initially but also from other areas without these nodules ("*de novo* HCC"). Dynamic CT and/or MRI were also performed in cases with hepatic nodules detected by US, liver cirrhosis, a tendency of tumor marker elevation, and difficult evaluation of the liver parenchyma by US. All the 127 patients were followed-up for 3 years after the initial gadoxetic acid-enhanced MRI examination. When imaging modalities led to diagnosis of HCC, recognizing hypervascularization by more than one experienced radiologist and other imaging modalities was regarded as the time of diagnosis of HCC. When needle biopsy was performed to investigate nodules, the time of diagnosis of HCC was when the

pathologists and physicians examined pathological tissue and diagnosed as HCC.

MRI

MRI was performed using a superconducting magnet that operated at 1.5 Tesla (Sigma EXCITE HD; GE Medical Systems, Milwaukee, WI) and an 8-channel phased-array coil. First, we obtained fast spoiled gradient-echo T1-weighted images (T1WIs) with dual echo acquisition and respiratory-triggered fat-saturated fast spin-echo T2-weighted images (T2WIs). Dynamic fat-suppressed gradient-echo T1WIs were obtained using a three-dimensional (3D) acquisition sequence before (precontrast) and 20-30 s, 60 s, 2 min, 5 min, 10 min, and 20 min after the administration of gadoxetic acid (Primovist; Bayer Schering Pharma, Berlin, Germany). This contrast agent (0.025 mmol/kg body weight) was administered intravenously as a bolus at a rate of 1 mL/s through an intravenous cubital line (20–22 gauge) that was flushed with 20 mL saline from a power injector. The delay time for the arterial phase scan was adjusted according to a fluoroscopic triggering method (20). All images were acquired in the transverse plane. Sagittal plane T1WIs were also obtained during the hepatocyte phase at 20 min after the injection of the contrast agent.

Statistical analysis

All continuous values are expressed as median (range). Fischer's exact probability test was used for comparisons between categorical variable and the non-parametric Mann-Whitney test was used to compare differences between continuous variables. Baseline clinical characteristics, including blood test results, were evaluated within 1 month of the initial MRI. We investigated whether or not HCC development was

associated with age, gender, fibrosis, etiology (HBV or HCV), platelet count, serum alanine aminotransferase (ALT), γ-glutamyl transpeptidase (γ-GTP), alpha-fetoprotein (AFP), and the presence or absence of hypovascular hypointense nodules.

Cumulative HCC development was estimated according to the Kaplan-Meier method and differences in the curves were tested using the log-rank test. Risk factors for HCC development were determined according to the Cox proportional hazard model. Subgroup analyses with a Cox proportional hazard model were applied to estimation of the hazard ratio (HR) of the non-clean liver group versus clean liver group in the dichotomized subgroups. All statistical analyses were performed using JMP software, version 10 (SAS Institute Japan, Tokyo, Japan). A two-sided p value <0.05 was considered statistically significant.

RESULTS

Characteristics of the patients and nodules

A total of 127 patients were enrolled, of whom 26 had chronic HBV infections and 101 had HCV infections, and 68 had virus-associated cirrhosis. No statistically significant differences in the initial clinical characteristics were found between the non-clean liver and clean liver groups (Table 1). Thirty five hypovascular hypointense nodules were found in 18 patients in the non-clean liver group (1–5 nodules per patient) at baseline (data not shown). Twenty-four of these 35 nodules were detectable only on the hepatocyte phase MRI and were undetectable by US, CT and non-hepatocyte phase MRI. None of the 35 nodules showed high intensity on T2WIs. The median nodule diameter was 8 mm (range: 4–13 mm, 33 nodules with 10mm or less, 2 nodules with 12 mm and 13 mm).

HCC incidence according to initial MRI findings

HCC was diagnosed in 17 patients, 10 in the non-clean liver group and 7 in the clean liver group; 14 of these patients had HCV infection. Thirteen patients were diagnosed according to the AASLD imaging criteria (19). Four patients were diagnosed pathologically by liver biopsies that were performed, based on enlargement of the nodules of >10 mm in diameter during the observation period.

The cumulative 1-, 2-, and 3-year HCC incidence rates were 1.5%, 10.2%, and 13.4%. As determined by the Kaplan-Meier method, these rates were 11.1% (95% confidence interval [CI], 0.0-25.6%), 38.8% (95% CI, 16.3-61.4%), and 55.5% (95% CI, 32.6-78.5%) in the non-clean liver group and 0.0% (95% CI, 0.0-2.3%), 5.5% (95%

CI, 0.0-9.8%), and 6.4% (95% CI, 1.8-11.0%) in the clean liver group; the former group showed significantly higher rates of development of typical HCC than the latter ($p < 0.001$) as shown in Figure 2. The median imaging intervals were 3 months (3-6 months) in the non-clean liver group and 4 months (2-12 months) in the clean liver group. The imaging interval of the non-clean liver group was shorter than clean liver group (3 vs. 4 months: $p = 0.015$). The median intervals between the initial MRI and HCC diagnosis was 16 months (9-32 months) in the non-clean liver group and 21 months (16-35 months) in the clean liver group.

In 11 of 17 patients with HCC development, HCCs developed at sites in which no nodules had been seen on the initial gadoxetic acid-enhanced MRI, *i.e. "de novo* HCC". These HCCs were found 4 in 18 patients in the non-clean liver group (3-year HCC incidence rates: 22.2%, 95% CI, 4.3-51.0%) and 7 in 109 patients in the clean liver group (3-year HCC incidence rates: 6.4%, 95% CI, 1.8-11.0%). The incidence rates of "*de novo* HCC" was significantly higher in the non-clean liver group than the clean liver group ($p = 0.003$, Figure 3). In the remaining 6 patients, HCCs developed at the same site of the initial nodules exclusively in 18 patients of a non-clean liver group by definition, and those HCCs arose among the nodules ≥8 mm in the initial MRI study.

Risk factors for HCC development

Univariate analyses showed that the significant risk factors for HCC development included older age ($p = 0.039$), cirrhosis ($p = 0.009$), a low platelet count ($p = 0.003$), a high AFP concentration ($p = 0.006$), and a non-clean liver ($p < 0.001$). Multivariate analysis with these variables revealed that older age (HR: 1.08; 95% CI, 1.01–1.16: $p = 0.024$), a low platelet count (HR 1.17; 95% CI, 1.03–1.35: $p = 0.017$), and a non-clean